Numerical Modeling of a 2 K J-T Heat Exchanger Used in Fermilab Vertical Test Stand VTS-1

Prabhat Kumar Gupta[a,*,1], Roger Rabehl[b]

[a]Cryo-Engineering and Cryo-Module Development Section, Raja Ramanna Centre for Advanced Technology (RRCAT), Indore (MP), India

[b]Test and Instrumentation Department, Technical Division, Fermi National Accelerator Laboratory, Batavia, IL, USA

Abstract

Fermilab Vertical Test Stand-1 (VTS-1) has been in operation since 2007 for testing superconducting radio frequency (SCRF) cavities at 2 K. This test stand includes a heat exchanger consisting of a single layer; helically wound finned tube, upstream of the J-T valve. A finite difference thermal model has been developed in Engineering Equation Solver (EES) to study the thermal performance of this heat exchanger during refilling of the test stand. The model can predict heat exchanger performance under various other operating conditions and is therefore useful as a design tool for similar heat exchangers in other facilities. The present paper discusses the different operational modes of this heat exchanger and its thermal characteristics under these operational modes. Results of this model have been compared with experimental data gathered from the VTS-1 heat exchanger, and they are in good agreement with the present model.

Keywords: 2 Kelvin J-T Heat Exchanger, Vertical Test Stand Operation, 2 Kelvin Refrigeration Systems

[*] *Corresponding author: Prabhat Kumar Gupta*

Email addresses: Prabhat Kumar Gupta (prabhat@rrcat.gov.in), Roger Rabehl (rabehl@fnal.gov)

[1] *Work reported in this article is conducted during the stay of first author at Fermilab as a Guest Cryogenic Engineer*

1. Introduction

Vertical Test Stand-1 (VTS-1) [1] at Fermilab is used to test superconducting radio frequency (SCRF) cavities in a 2 K liquid helium bath.The test stand includes a J-T heat exchanger consisting of a single layer of coiled, finned tubing. Other test stands such as Fermilab's Vertical Magnet Test Facility (VMTF) [2] and DESY's Tesla Test Facility (TTF) Vertical Cryostat [3] have also used similar single-layer J-T heat exchangers for testing superconducting magnets and SCRF cavities, respectively.

A J-T heat exchanger in a 2 K refrigeration system transfers heat from the liquid helium supply to the returning low pressure helium vapor, cooling the liquid to near 2.2 K before it expands through the downstream J-T valve as shown in Figure 1. Flashing losses are minimized.

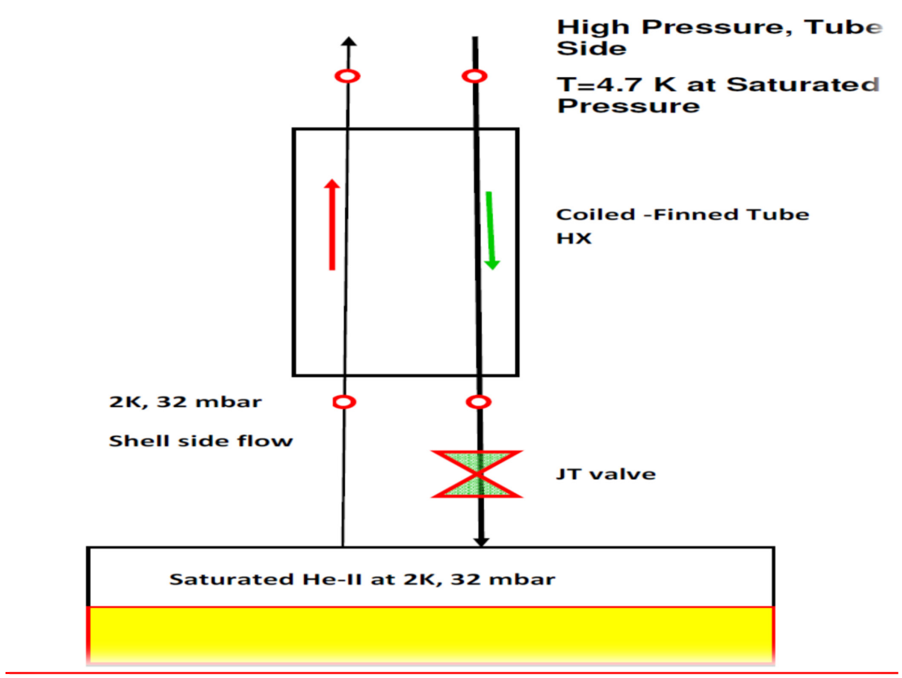

Figure 1. J-T heat exchanger flow scheme

In VTS-1, SCRF cavities are immersed in 2 K liquid helium in a vessel as shown in Figure 2.

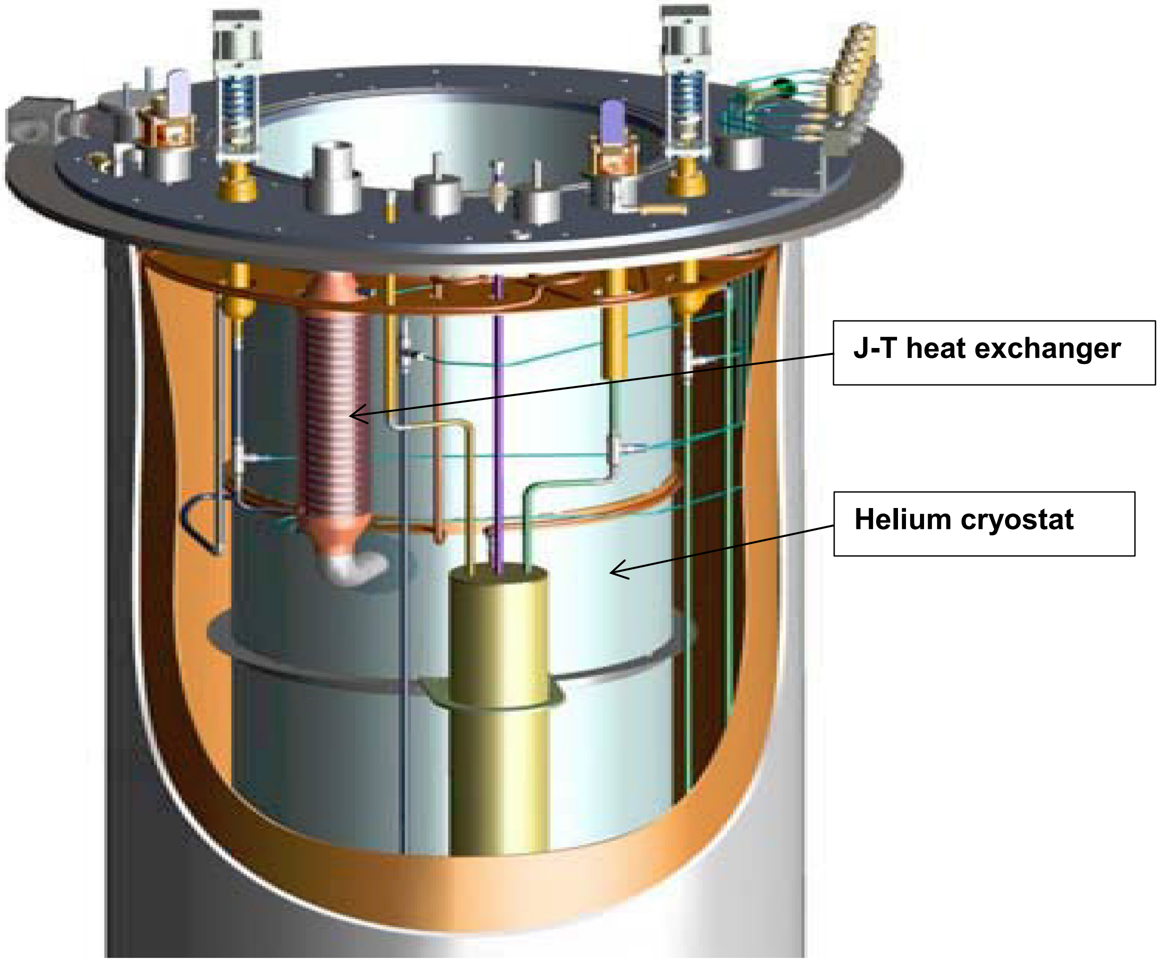

Figure 2. Vertical Test Stand (VTS-1) solid model showing the J-T heat exchanger and the helium cryostat

There may be different modes of filling the cryostat, and liquid flashing losses are dependent on these modes.

- A serial fill and pump-down achieves a low liquid level at 2 K. Approximately 50% of the accumulated 4.5 K liquid vaporizes during the pump-down to 2 K. In this mode of filling, the 2 K liquid is achieved at the cost of high flashing losses. The result is a cryostat only half-filled with 2 K liquid. A J-T heat exchanger provides no benefit in this mode.

- A concurrent fill and pump-down achieves a very high liquid level at 2 K. Pump-down to 2 K is started when the cryostat is only partially filled with liquid helium, and filling continues throughout the pump-down in order to achieve a high liquid level at 2 K. The J-T heat exchanger is used during this mode of filling to cool the liquid helium supplied to the cryostat thereby reducing the required 4.5 K liquid helium transfer and decreasing the time required to reach 2 K.
- A continuous fill maintains a steady liquid level during 2 K operation. Upon achieving 2 K, cavity tests are performed and the liquid level begins to drop at a rate depending on the power dissidpated in the liquid bath. Therefore during continuous high-power testing of SCRF cavities, constant liquid level has to be maintained by a continuous liquid supply. The J-T heat exchanger minimizes the flashing losses of this liquid supply.

During a concurrent fill and pump-down, the J-T heat exchanger is operated in an unbalanced mass flow rate condition. The tube-side flow is greater than the shell-side flow. During a continuous fill, there are equal flow rates in the tube side and the shell side of the heat exchanger. In these different modes of operation, the total heat capacities of the streams are different due to unbalanced mass flow rates and strong variations in helium thermo-physical properties over the operating temperature range. Therefore the J-T heat exchanger will behave differently in these operational modes. In the present study, a finite difference model is developed in Engineering Equation Solver (EES) to analyze the temperature distribution of the heat exchanger and its operational characteristics in each operational mode. The results of this model are compared with experimental results gathered from the in-service J-T heat exchanger of VTS-1.

2. Description of VTS-1 J-T Heat Exchanger

The VTS-1 J-T heat exchanger is a single-layer, coiled, finned tube heat exchanger as shown in the VTS-1 cut-away view of Figure 2. It consists of a single layer of finned copper tube helically wound on a polyethylene mandrel, called the inner core. This subassembly is jacketed by a stainless steel pipe, called the outer core. The dead space between two consecutive coils is filled by nylon-reinforced cotton cord. The complete assembly of this heat exchanger is shown in Figure 3. Other geometric parameters of this heat exchanger are given in Table 1.The 4.7 K saturated liquid passes through the helically-wound finned tube from top to bottom. The outer shell of this heat exchanger is directly connected to the helium vessel as can be seen in Figure 2, and therefore sub-atmospheric cold helium gas passes over the finned tubes in a cross-flow pattern and exchanges heat with the incoming saturated liquid before exiting to the test stand pumping line.

Figure 3. Picture of the J-T heat exchanger used in VTS-1.

Table 1.Geometric parameters of the J-T heat exchanger

Geometric parameters of the helically-wound, finned copper tube	Tube inner diameter, di	7.74 mm
	Fin outer diameter, d_f	22.25 mm
	Height of fins, h_f	6.35 mm
	No. of fins per inch, n	8
Geometric parameters of the J-T heat exchanger	Total axial length of heat exchanger assembly	578.0 mm
	Actual length with finned tubes, L	488.0 mm
	Mean diameter, D_e	86.0 mm

3. J-T Heat Exchanger Modeling

To simulate the heat transfer characteristics of a J-T heat exchanger, partial differential equations describing the temperature profiles of the hot and cold streams with no heat generation in the fluids and with no external heat loads have been formulated. These equations coupled with the counter-flow heat transfer process can be written as follows:

$$Hot\ fluid: \quad \dot{m}_h c_{ph} \frac{dT_h}{dx_h} + U \frac{A_h}{L}(T_h - T_c) = 0 \quad (1)$$

$$Cold\ fluid: \quad \dot{m}_c c_{pc} \frac{dT_c}{dx_c} + U \frac{A_c}{L}\left(T_c - T_h\right) = 0 \quad (2)$$

where $\dot{m}_h$ and $\dot{m}_c$ are the mass flow rates of the hot and cold streams, c_{ph} and c_{pc} are the specific heats of the respective fluids, U is the overall heat transfer coefficient between the two fluid streams ,A_h and A_c are the heat transfer areas for the tube side and the shell side, L is the actual finned tube axial length of the heat exchanger , T_h and

T_c are the tube side (hot fluid) and shell side (cold fluid) temperatures, x_h and x_c are the fluid path lengths for the respective fluids. Because the fluid path lengths are different, Equations 1 and 2 must be normalized by the relation of Equation 3:

$$dx_h = l_h \frac{dx_c}{L} \quad (3).$$

where l_h is the total length of finned tubes wound on the inner core.

The perimeter of the inner tube surface (surface area per unit axial length, $\frac{A_h}{L}$), S_i, is given by Equation 4:

$$S_i = \pi^2 \frac{D_e}{d_f} d_i \quad (4).$$

The perimeter of the outer finned surface (surface area per unit axial length, $\frac{A_c}{L}$), S_o, is given by Equation 5 :

$$S_o = \pi^2 \left[\frac{n}{2}\left(d_f^{\,2} - d_o^{\,2}\right) + d_o(1 - tn) + d_f \cdot t \cdot n \right] \frac{D_e}{d_f} \quad (5).$$

Free flow area offered by the fin arrangement, A_{fc}, is given by Equation 6:

$$A_{fc} = \pi D_e \left[(d_f - d_o)(1 - nt) \right] \quad (6).$$

The surface area offered by the outer finned surface in one coil, A_s, is given by Equation 7:

$$A_s = \pi^2 \left[\frac{n}{2}\left(d_f^{\,2} - d_o^{\,2}\right) + d_o(1 - tn) + d_f \cdot t \cdot n \right] D_e \quad (7).$$

The shell-side Reynolds number Re_s is based on the total cross-section area available for shell-side flow and can be calculated as shown in Equation 8:

$$\mathrm{Re}_s = \frac{\dot{m}_c D_h}{A_{fc}\mu} \quad \text{……………………………………………………………………………………(8).}$$

The characteristic dimension for the Reynolds number in Equation 8 is the equivalent diameter, or the hydraulic diameter D_h, as calculated by Equation 9:

$$D_h = \frac{4A_{fc}}{A_s / L} \quad \text{…………………………………………………………………….. (9).}$$

The mass flow rate per unit free-flow area, G, will be used for determining the heat transfer coefficients and is calculated by Equation 10:

$$G = \frac{\dot{m}_c}{A_{fc}} \quad \text{……………………………………………………………………….(10).}$$

In the above geometric formulae, $d_{i,}d_o$ and d_f are the inner, outer and finned tube diameters, respectively, and *t* is the fin thickness, and *n* is the number of fins per unit length. D_e is the mean diameter of the heat exchanger and it is defined as a mean diameter of a finned tube coil wrapped over the heat exchanger inner core.

The formulae presented above for calculating the geometric parameters for this kind of heat exchanger have been taken from the design procedures developed at RRCAT [4, 5].

The overall heat transfer coefficient, U, is calculated by Equation 11, assuming a fin efficiency of unity:

$$U = \frac{h_o h_i s_i}{h_o s_o + h_i s_i} \quad \text{……………………………………………………………….(11).}$$

Here h_i and h_o are the inner heat transfer coefficient and outer heat transfer coefficient. They are calculated using Equations 12 and 13 [5]:

$$h_i = 0.023\,\mathrm{Re}^{0.8}\,\mathrm{Pr}^{1/3}\left(\frac{k}{d_i}\right) \quad \text{……………………………………………………(12).}$$

$$h_o = 0.19\left(\frac{k}{d_o}\right)\mathrm{Re}_s^{\,0.703}\,\mathrm{Pr}^{1/3} \qquad (13).$$

Where Pr and Re are Prandtl number and the Reynolds number, respectively, and *k* is the fluid thermal conductivity.

To determine the temperature profiles across the heat exchanger, the heat exchanger energy equations (Equations 1 and 2) have been divided axially into *n* elements (typically more than 200 nodes) using the finite difference method. These equations are then converted into linear algebraic equations. The EES software package has been used to obtain the solution. The program developed in EES takes care of property variations along the length of the heat exchanger. Helium properties data used in the analysis have been calculated using the in-built subroutine of EES.

4. Effectiveness of J-T Heat Exchanger

The effectiveness of any heat exchanger is defined as the ratio of the actual heat transfer to the maximum possible heat transfer. In conventional heat exchangers used in room-temperature applications, the properties of fluids do not vary much with the temperatures and pressures. Therefore the effectiveness of any heat exchanger operating near this constant property zone can be expressed in terms of the heat exchanger end temperatures. However, the effectiveness of these heat exchangers operating in a variable property zone should be expressed in terms of the relevant enthalpy differences.

Typically, the maximum possible heat transfer occurs when the temperatures of the two fluids coincide at the outlet of the heat exchanger. However, due to variations in properties of helium, these two temperatures may coincide at another location within the heat exchanger. This location of minimum temperature difference between streams within the heat exchanger depends on the operating temperatures and pressures of each individual stream. For convenience, effectiveness in these heat exchangers is defined on the basis of end conditions of the heat exchanger, regardless of where the minimum temperature difference occurs inside the heat exchanger.

The effectiveness of these heat exchangers operating in the variable property zone can be defined on the basis of the minimum capacitance fluid. If the hot fluid is the minimum capacitance fluid, the effectiveness of these heat exchangers is defined by Equation 14:

$$\varepsilon_h = \frac{H_{h,in} - H_{h,out}}{H_{h,in} - H^*_{in}} \quad \ldots\ldots\ldots\ldots\ldots\ldots\ldots\ldots\ldots\ldots\ldots\ldots\ldots\ldots\ldots\ldots\ldots\ldots\ldots\ldots..(14).$$

where H^*_{in} is the hot fluid enthalpy at the cold fluid inlet temperature. Similarly if the cold fluid is the minimum capacitance fluid, the effectiveness of the heat exchangers is defined by Equation 15:

$$\varepsilon_c = \frac{H_{c,out} - H_{c,in}}{H^*_{out} - H_{c,in}} \quad \ldots\ldots\ldots\ldots\ldots\ldots\ldots\ldots\ldots\ldots\ldots\ldots\ldots\ldots\ldots\ldots\ldots\ldots\ldots\ldots\ldots (15).$$

where H^*_{out} is the cold fluid enthalpy at the hot fluid inlet temperature. For Equations 14 and 15, H_h and H_c are the hot fluid and cold fluid enthalpies at the respective points.

5. Results and Discussions

5.1. Experimental validation of model

The present model has been validated by comparing the theoretical results with the experimental data gathered from the VTS-1 J-T heat exchanger. Experimental data gathered during VTS-1 refills have been used for this comparison [6]. During these refills, liquid helium accumulated in the test dewar at rates ranging from 0.217-0.397 in/min. Liquid helium supply temperature ranged from 4.828-4.875 K. All four end temperatures were measured during these tests. Performance of the J-T heat exchanger during these 2 K refills of VTS-1 is documented elsewhere [6].

During refilling of the dewar, there is a mass imbalance in J-T heat exchanger. The liquid supply mass flow rate is greater than the gas return flow rate. The accurate calculation of these mass flow rates is important to determine the performance of the J-T heat exchanger. For calculation of the tube-side mass flow rate , $\dot{m}_h$, and the shell-side mass flow rate , $\dot{m}_c$, the flashing rate has been calculated using the four measured end temperatures of the heat exchanger, and then using the liquid fill rate of the test dewar both mass flow rates have been calculated. The average mass flow rate for the tube side is 13.29 g/s, and for the shell side it is 4.75 g/s during a 0.397 in/min filling of the VTS-1 cryostat.

Figure 4 shows the comparison between effectiveness calculated from measured data and predicted effectiveness for the existing heat exchanger in VTS-1. Figure 4 shows that predicted effectiveness is within 5% of measured values. Figure 4 also compares the predicted tube-side exit temperatures with the measured values and shows very good agreement.

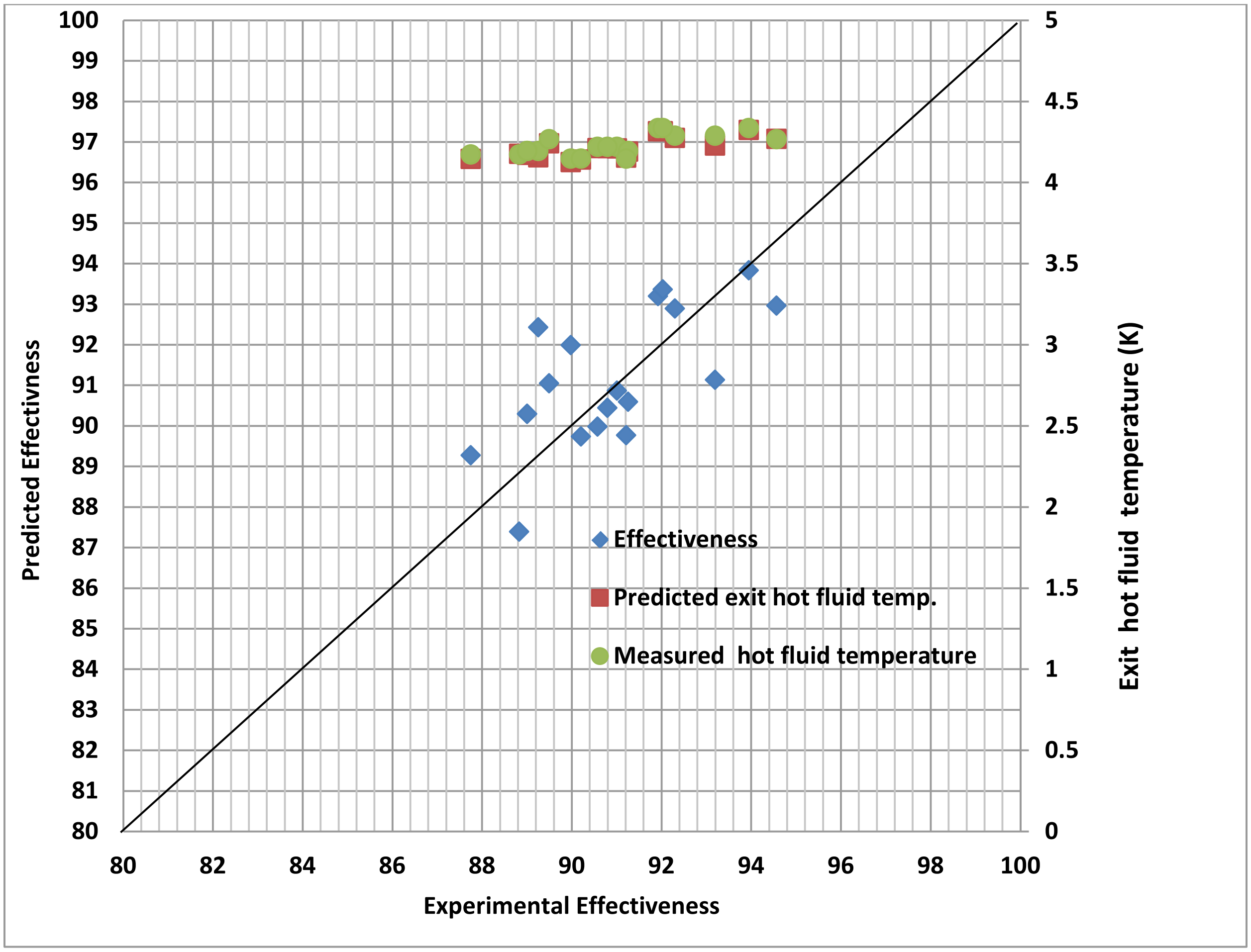

Figure 4. Comparison between experimental results and calculated results

5.2. Heat exchanger temperature profile studies under various operational modes

During filling of the 2 K bath, a larger fraction of the total mass flow rate will flow through the tubes and a smaller fraction of the total flow rate will flow through the shell side of the heat exchanger. This filling process of the 2 K bath will generate the mass flow rate imbalance in the heat exchanger. Therefore this mass flow rate imbalancing in the heat exchanger will influence the performance of the heat exchanger. Figure 5 shows that the specific heat of the shell-side stream is lower than the specific heat of the tube-side stream through most of the heat exchanger length, crossing at the cold end of the J-T heat exchanger prescribed temperature range.

Due to this mass flow rate imbalance in the heat exchanger (the tube-side mass flow rate is 13.29 g/s, and the shell-side mass flow rate is 4.75 g/s), the heat capacity ($\dot{m}c_p$) of the shell side is less than the heat capacity of the tube side throughout the heat exchanger length. This can be seen in Figure 6. Therefore the tube-side flow will experience less temperature change than the shell-side flow.

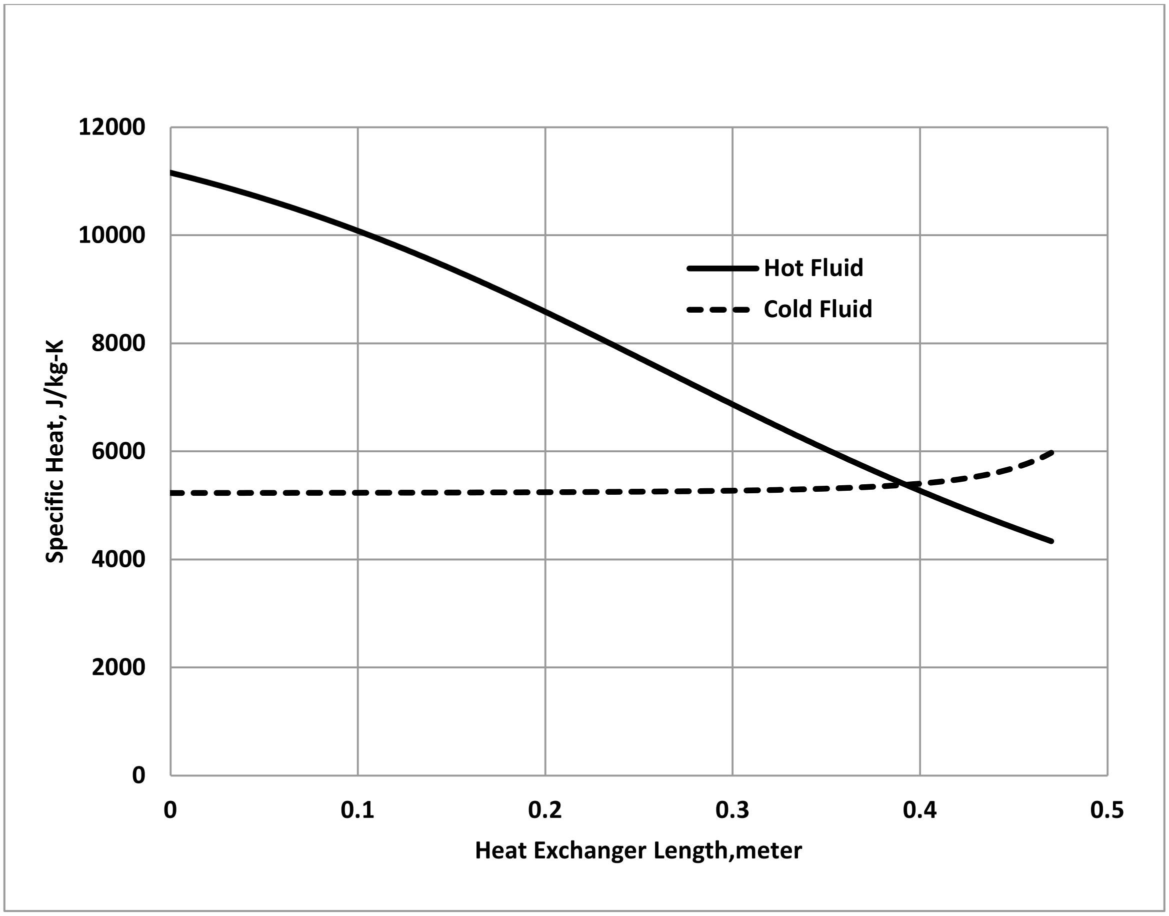

Figure 5. Variations in specific heat along the heat exchanger

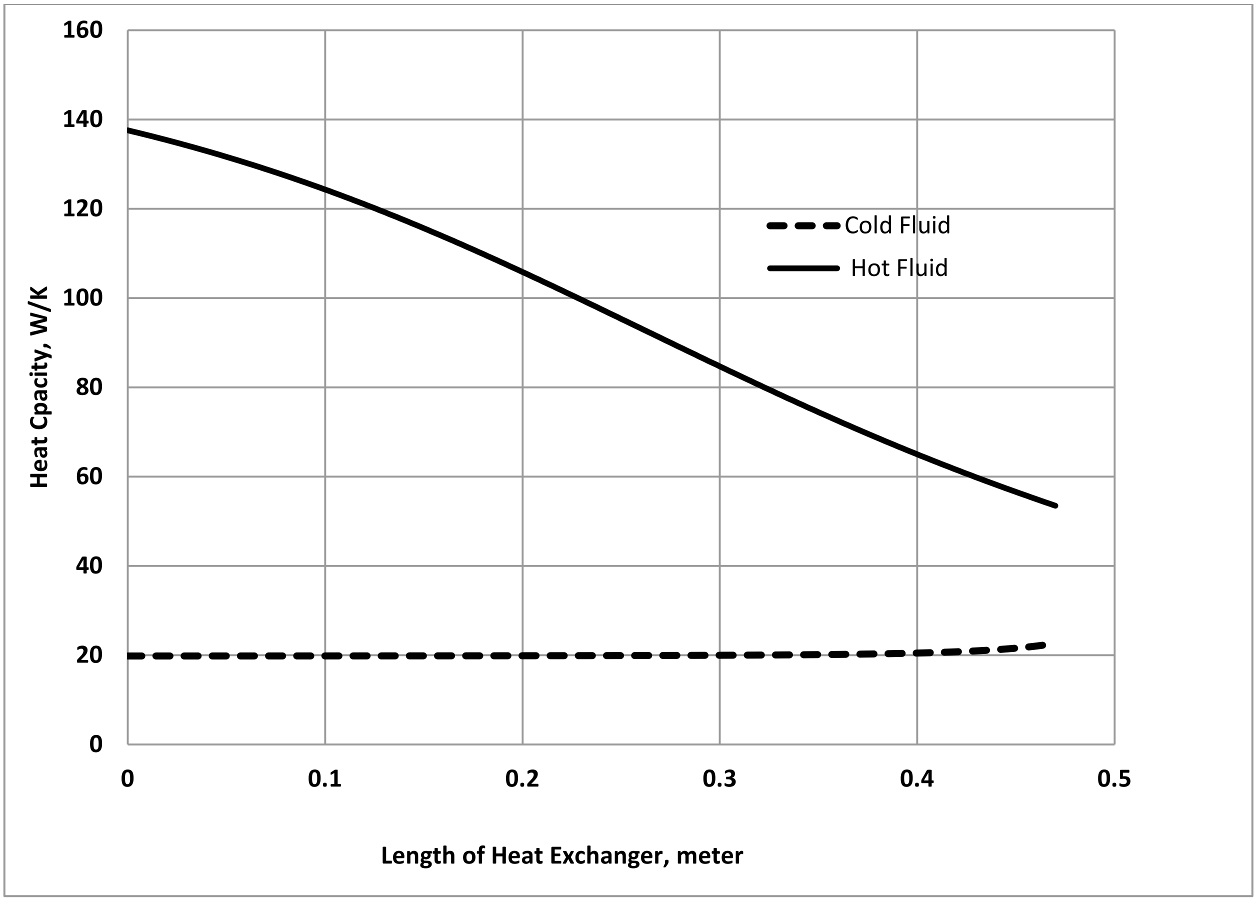

Figure 6. Variation in total heat capacity along the length of the heat exchanger

Figure 7 shows the calculated temperature profiles of the heat exchanger for the tube-side mass flow rate of 12.33 g/s and the shell-side mass flow rate of 3.79 g/s. Figure 7 clearly shows that the hot fluid experiences less temperature change throughout the length of the heat exchanger. The irreversibility generated by the flow imbalance and variable specific heats will prevent the heat exchanger from achieving the lowest temperature no matter how big the heat exchanger, as can be seen in Figure 8. Figure 8 shows the temperature profile of a heat exchanger which is almost double in length with the same other geometric dimensions.

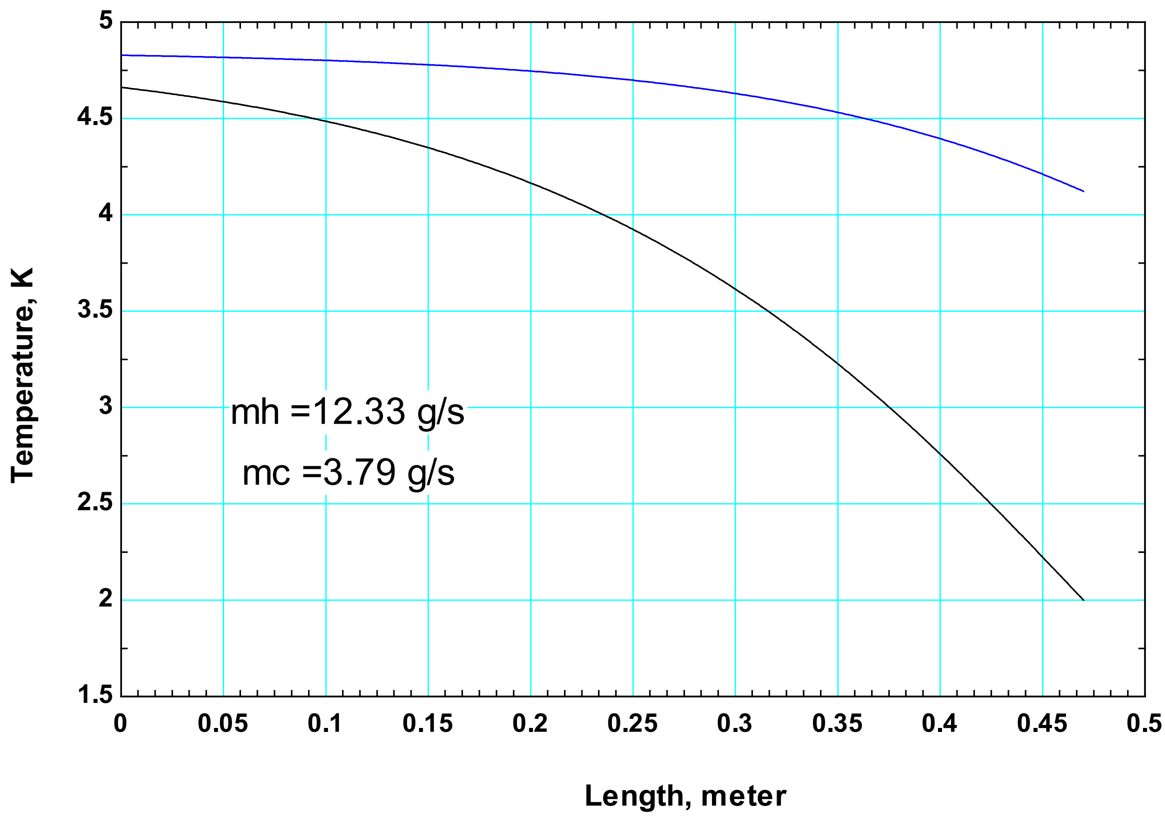

Figure 7. Temperature profiles of the heat exchanger during filling of VTS-1.

Figure 8 shows that there is a temperature pinch at the hot end and it can also be seen that the hot fluid temperature is lowered only to 4.064 K from 4.121 K despite the heat exchanger length being almost doubled. Therefore increasing the length of the heat exchanger is not providing any extra advantage to get the lower tube-side fluid temperature because of this flow rate imbalance in the heat exchanger. Here it could be concluded that even a bigger heat exchanger (larger surface area) would not be beneficial to increase the 2K liquid fraction in this mode of operation.

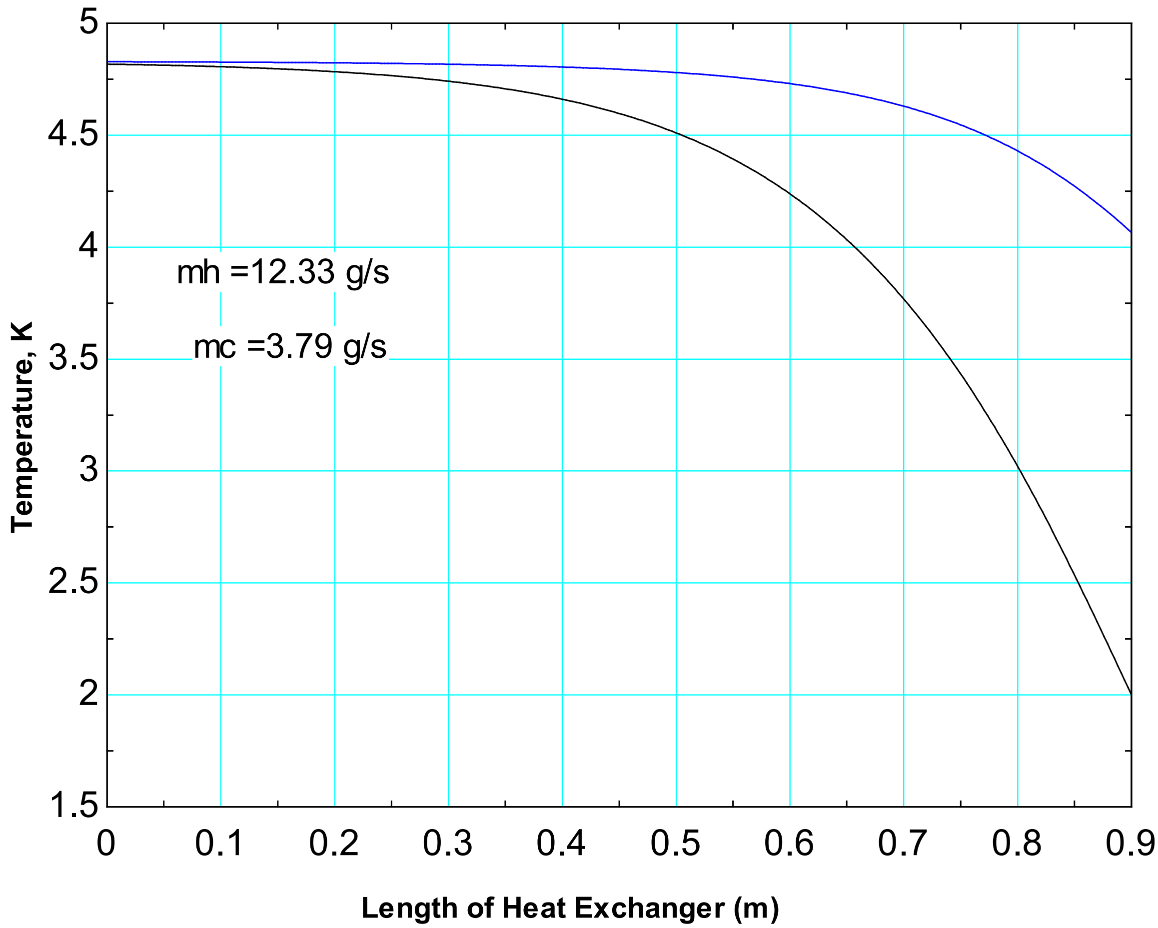

Figure 8. Heat exchanger length effect on temperature profiles during filling mode

On the contrary while maintaining a constant liquid level, 2 K liquid has to be supplied constantly to the test dewar during dissipation of power. Equal mass flow rates will flow through the tube and shell sides of the heat exchanger to maintain a constant liquid level in the 2 K bath. Therefore in this mode of operation, there would not be any mass flow imbalance and only variations in specific heat along the heat exchanger, as shown in Figure 5, will govern the performance of the heat exchanger. Figure 9 shows the temperature profiles of the same heat exchanger during this mode of operation. Here it can be noted that the same heat exchanger is capable of lowering the liquid helium temperature to 2.48 K compared to the 4.121 K (Figure 7) calculated while operating in filling mode.

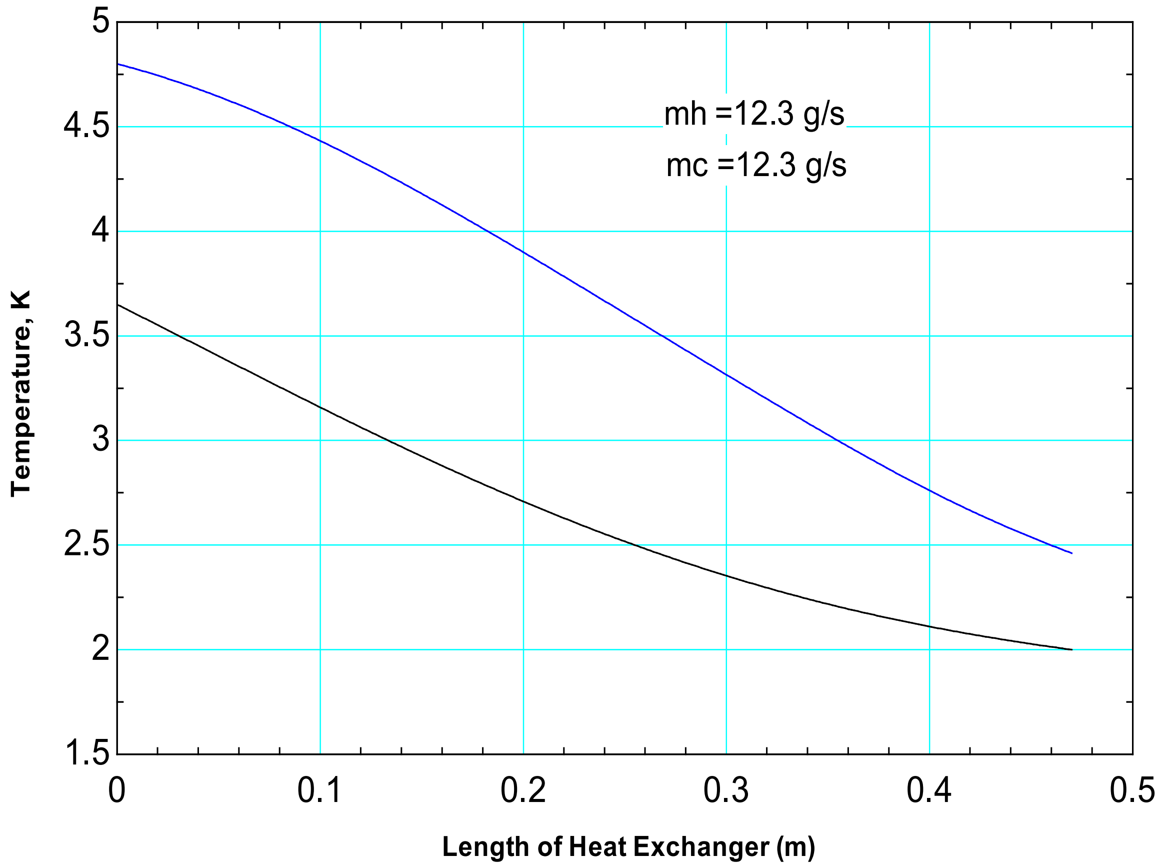

Figure 9. Temperature profiles of the heat exchanger during refilling to maintain the constantliquid level in VTS

Figure 10 shows the temperature profiles for the longer heat exchanger (0.7 m). It can be seen that liquid helium temperature is dropped to 2.189 K as the heat exchanger length increased. Hence in this mode of operation, liquid helium temperature would be closer to the bath temperature as heat exchanger length increases and pressure drop would be the only limiting factor to optimize the length of the heat exchanger. During this mode of operation, using the heat exchanger would significantly increase the 2 K liquid yield as the liquid helium temperature would be much lower before the J-T valve.

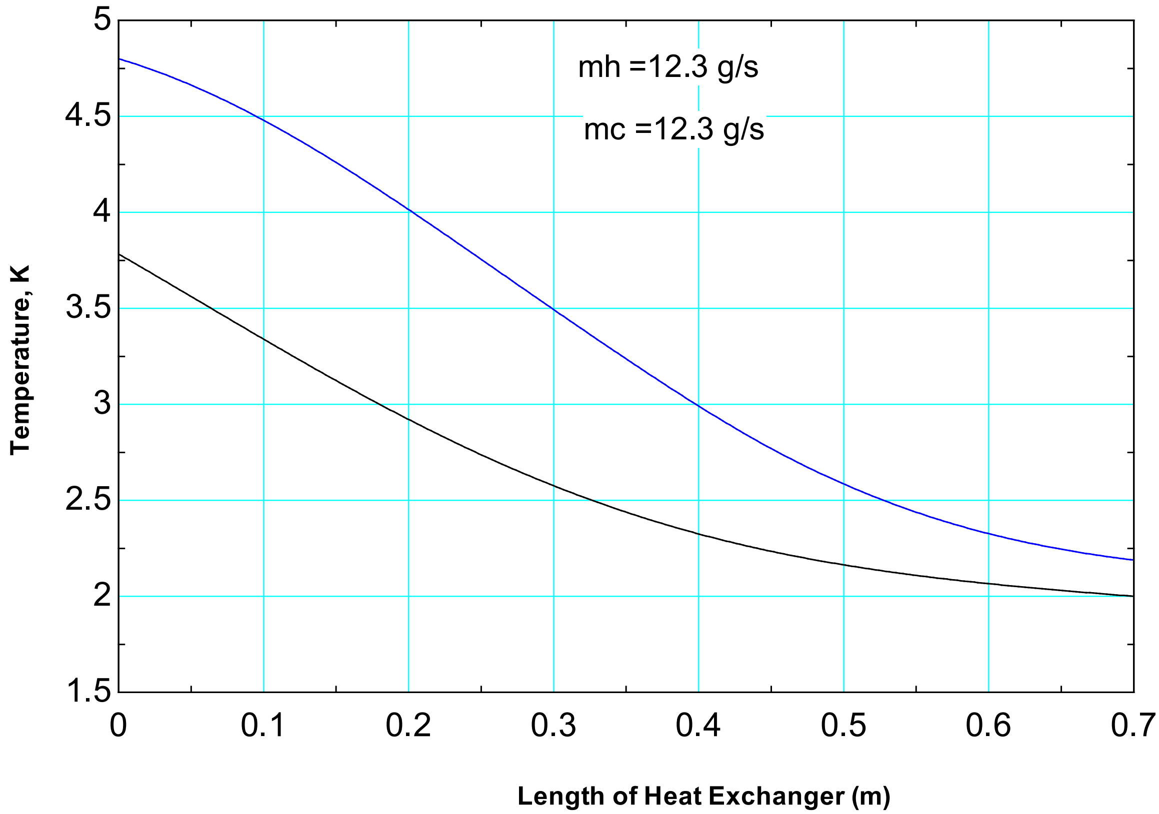

Figure 10. Temperature profiles of longer heat exchangers during refilling to maintain the constant liquid level in VTS-1.

5.3. Heat exchanger sizing effect on flash reduction

This section presents the heat exchanger sizing effect on vapor flash reduction during filling of the test dewar. It is assumed that the test dewar is filling at the rate of 0.397 in/min, and the liquid helium supply temperature is 4.8 K. To calculate the relative reduction in flashed vapor flow rate, vapor fraction is calculated with and without a J-T heat exchanger in the system. Therefore, percent relative flash reduction can be expressed by Equation 16:

$$\frac{\Delta m_v}{m_h} = (X_{noHX} - X_{HX}) \times 100 \quad \text{.......(16).}$$

where X_{noHX} is the quality of liquid entering the VTS-1 cryostat without a J-T heat exchanger, X_{HX} is the quality of liquid entering the VTS-1 cryostat with a J-T heat exchanger, and $\Delta\, m_v$ is the change in vapor flash.

Figure 11 shows the percent relative flash reduction vs. heat exchanger length. It could be noted that there is 21.5 % reduction in flashed vapor as compared to if there is no heat exchanger in the system. It can also be seen from Figure 11 that if the heat exchanger length is increased beyond 0.7 m; there is very little gain in flash reduction. This is because of unbalanced operation of the heat exchanger as described in the previous section. Figure 11 also shows that the effectiveness of the heat exchanger increases with the length of the heat exchanger. The effectiveness of a heat exchanger increases because the hot end temperature of the heat exchanger gets pinched due to its unbalanced operation. Here it can be stated that high effectiveness of this heat exchanger is not a true performance parameter for this mode of operation.

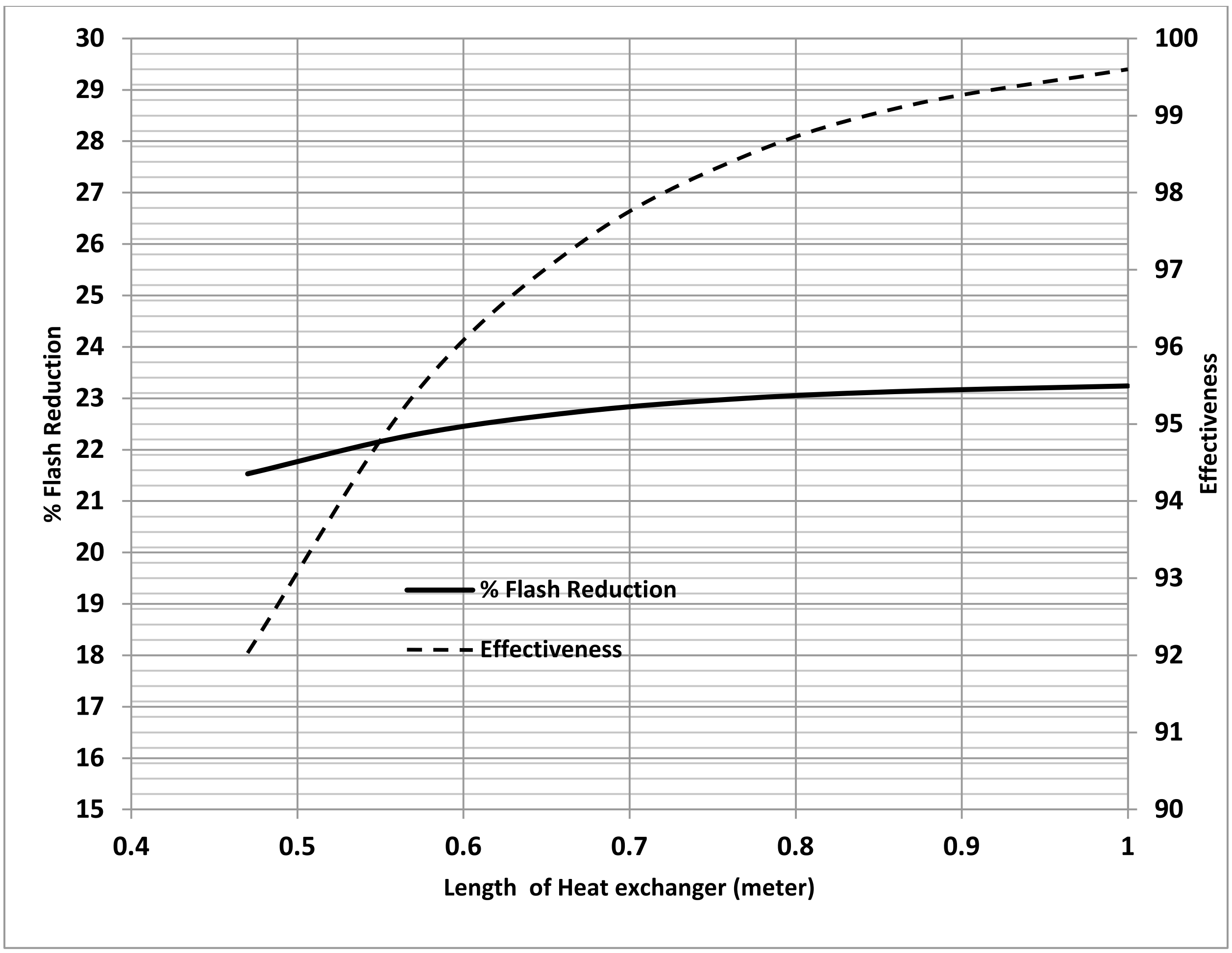

Figure 11. Percent relative flash reduction for varying heat exchanger length during filling mode.

5.4. Shell-side inlet temperature effect

Figure 12 shows the effect of shell-side inlet temperature of the heat exchanger on relative vapor flash reduction for a filling rate of 0.397 in/min. Figure 12 shows that if the inlet temperature is 2 K, there is a 21.5 % reduction in vapor flashing, and if the inlet temperature rises to 2.8 K there is only a 15.4 % reduction in vapor flashing. This happens due to a rise in the temperature before the J-T valve from 3.978 K to 4.3 K.

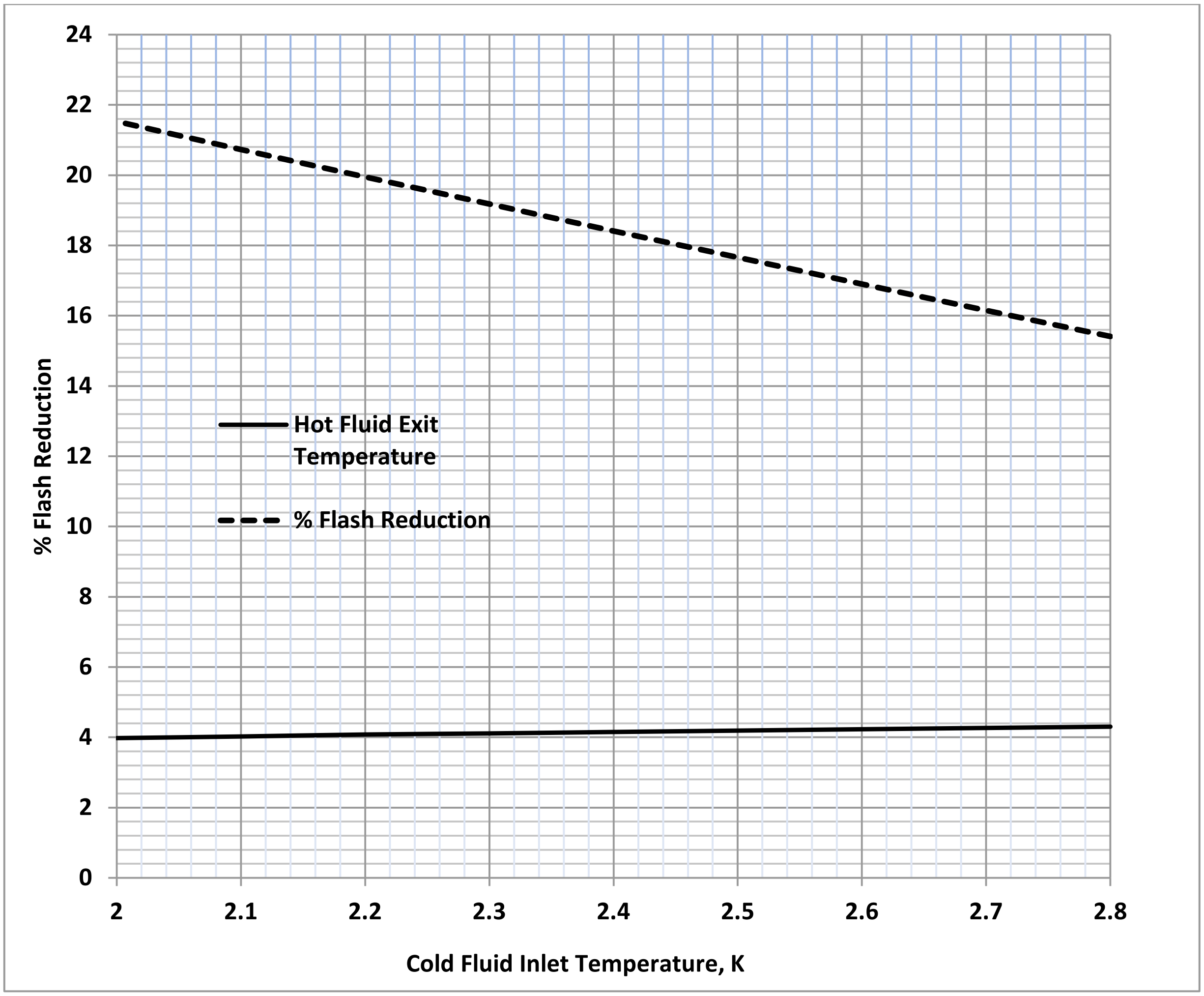

Figure 12. Effect of heat exchanger shell-side inlet temperature on relative vapor flash reduction

5.5. Tube-side inlet temperature effect

Figure 13 shows the effect of the tube-side inlet temperature (liquid helium supply temperature) on vapor flash reduction during filling of VTS-1. Figure 13 shows that if the liquid supply temperature is 4.3 K, there is a 32.41% reduction in vapor flashing as compared to if there is no heat exchanger in the system. As this supplied liquid saturated temperature increases, percent flash reduction decreases due to a rise in the temperature before the J-T valve. There is only a 21.5% flash reduction if the liquid supply temperature is 4.82K, and the liquid temperature will drop to only 3.978 K in the J-T heat exchanger as can be seen in Figure 13.

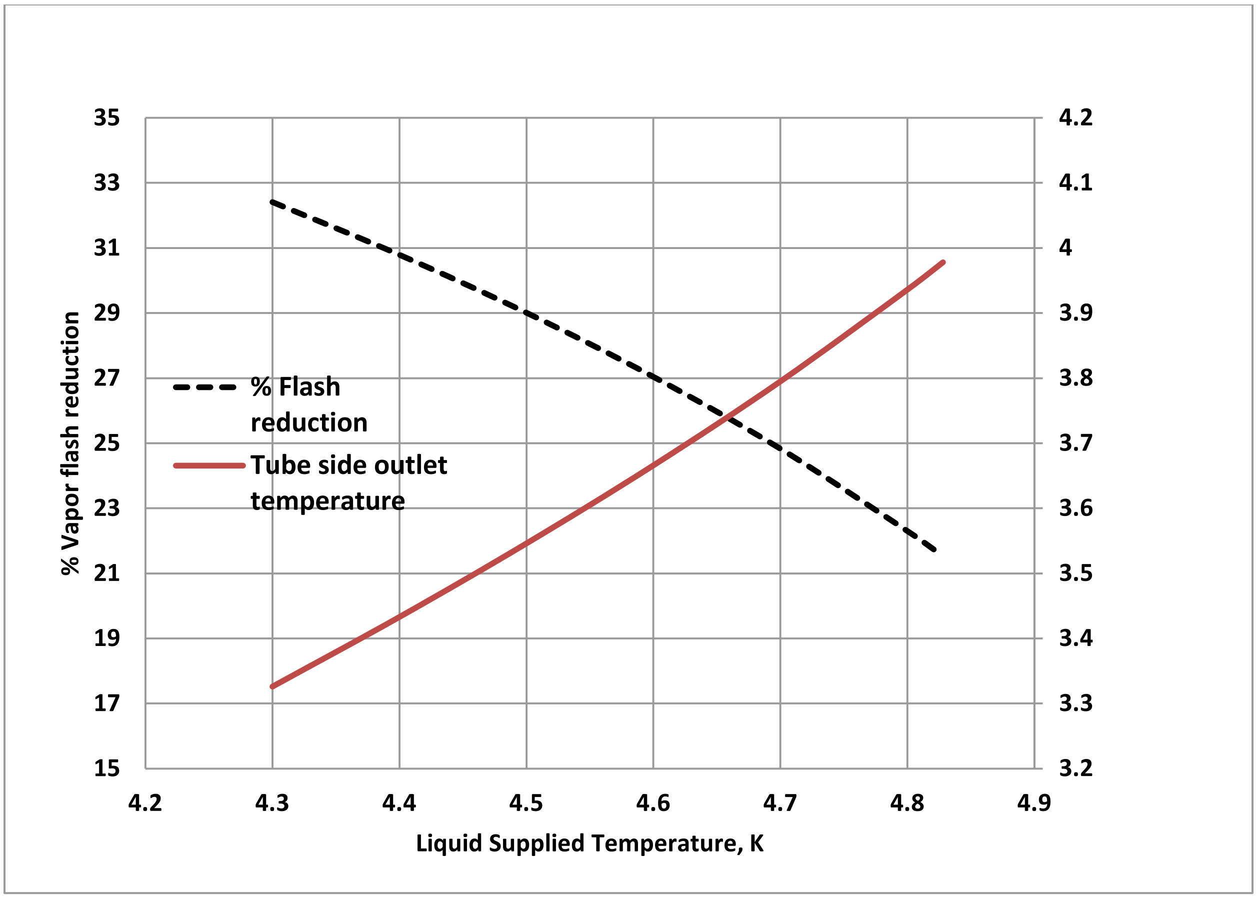

Figure 13. Effect of liquid helium supply temperature on vapor flash reduction

6.0. Conclusions

A finite difference based J-T heat exchanger model has been developed. Results obtained from the model are in good agreement with the experimental results. The present study shows that J-T heat exchanger performance characteristics are different in different modes of operation and play an important role in vapor flash reduction. The study also provides the interesting results that heat exchanger sizing can play an important role while maintaining constant liquid level in the test dewar by significantly reducing vapor flashing. However, heat exchanger length does not play a significant role while filling the test dewar due to unbalanced operation of this heat exchanger.

This study also quantifies the effect of heat exchanger tube-side and shell-side inlet temperatures on the percent vapor flash reduction. The presented developed model will serve as a useful tool to design similar heat exchangers for future needs.

Acknowledgments:

The Fermi National Accelerator Laboratory is operated by Fermi Research Alliance, LLC under Contract No. De-AC02-07CH11359 with the United States Department of Energy.

The VTS-1 Test Stand is operated by Fermilab's Technical Division/Test &Instrumentation Department. Solid modeling was provided by Clark Reid of Fermilab's Technical Division/Design & Drafting Department.

References:

[1].J. P. Ozelis, et. al., Design and Commissioning of Fermilab's Vertical Test Stand for ILC SRF Cavities, Proceedings of the 22nd Particle Accelerator Conference (PAC'07): 2283-2285

[2].T. J. Peterson, R. J. Rabehl, and C. D.Sylvester, A 1400 liter 1.8 K test facility.Advances in Cryogenic Engineering, 1998; Vol. 43 A :541-548.

[3].G. Grygiel, R. Lange, T.Nicol, B. Petersen,T. Peterson, D. Sellman,D.Trines. Cryogenic performance of the first vertical dewarof the tesla test facility.TESLA-Report 1994-25, source: http://flash.desy.de/reports_publications

[4].Gupta Prabhat Kumar, Kush PK,Tiwari A. Design and optimization of coil finned-tube heat exchangers for cryogenic applications.Cryogenics,2007;47:322-332.

[5].Gupta Prabhat Kumar, Kush PK, Tiwari A. Experimental research on heat transfer coefficients for cryogenic cross-counter flow coiled finned tube heat exchangers. Int. Journal of Refrigeration 2009, Vol. 32, no. 5, p. 960 – 972.

[6].R. Rabehl, "J-T Heat Exchanger Performance During a 2 K Refill of VTS-1," T&I Department Note TID-N-72, July 2009.